COMPUTATIONAL DESIGN-TO-FABRICATION USING SPATIAL GRAMMARS: AUTOMATICALLY GENERATING PRINTABLE CAR WHEEL DESIGN VARIANTS

Chen, Tian; Shea, Kristina
Swiss Federal Institute of Technology in Zurich, Switzerland

Abstract

Additive Manufacturing (AM) technologies offer new possibilities for engineers to fabricate designs that may not otherwise be possible or cost-effective with conventional methods. However, each process has constraints that must be adhered to and designers faced with such freedom do not readily explore the new search space offered. Computational design-to-fabrication, introduced in this paper, utilizes new AM opportunities by encoding the constraints of AM processes as well as considerations such as style and performance, into generative design systems that automatically generate designs that are directly printable. This paper presents the specific example of generating car wheel spoke variants using a set of 12 spatial grammar rules that conform to the DfAM constraints for the Fused Deposition Modeling printer UPrint SE Plus and FEM meshing and analysis requirements. From a set of 72,500 valid designs, 100 were generated automatically, 12 of which are fabricated. The results demonstrate the spatial grammar's capability to automatically generate valid designs, both known and new to spark creativity, that can also be directly analyzed with FEM and fabricated using 3D printing.

Keywords: Computational design synthesis, Design for Additive Manufacturing, Spatial grammar, Design methods

Contact:
Tian Chen
Swiss Federal Institute of Technology in Zurich
Engineering Design and Computing Laboratory, D-MAVT
Switzerland
ttc@ethz.ch

Please cite this paper as:
Surnames, Initials: *Title of paper*. In: Proceedings of the 20th International Conference on Engineering Design (ICED15), Vol. nn: Title of Volume, Milan, Italy, 27.-30.07.2015

1 INTRODUCTION

Additive manufacturing (AM) technologies offer a new realm of possibilities for engineers to design and fabricate products that would not otherwise be possible or cost-effective with conventional methods such as machining, injection molding or casting. Developments in the fields of parametric modeling and generative design as well as computational design optimization are well placed to help designers take advantage of these new capabilities through generation of innovative and directly printable solutions. Such designs can, e.g., incorporate complex geometry, integrate parts, have a unique customization or personalization and optimize material use.

While AM offers many new capabilities, there exist constraints as with any fabrication technology. Doubrovski (2011) mentions the existence of fabrication constraints while stating that for meso- and microstructures, the success of fabrication depends on the resolution or process-dependent variables. Meisel and Williams (2014) carry out studies of the Polyjet material jetting process to determine minimum printable feature sizes and the overhang angle at which printed parts are self-supporting and no longer require support material. Dimitrov (2006) investigates the achievable dimensional and geometric accuracy of binder jetting processes (3DP) by fabricating a cubic part with different sized extrusions and cutouts. Each AM process and machine type has a different set of dimensional constraints related to the process, build material, support material when used, and post-processing. Mechanical properties also vary and are tested in the literature but are beyond the scope of this paper.

Computational design-to-fabrication aims to take advantage of the new opportunities of AM by encoding the constraints of a particular AM process and machine type so as to automatically generate and optimize designs directly for this process, including single parts and assemblies. Through this, only valid designs that can be directly and automatically printed are generated. This goes beyond the conventional paper-based approach of providing guidelines for Design for Additive Manufacture (DfAM), e.g. as found on many AM websites, and also reduces the common trial-and-error process of designing for them. Further, it is argued here that including AM constraints upfront in the design generation process results in more suitable designs compared to, say, continuous topology optimization methods that often only consider fabrication constraints in the post-processing stage by, e.g., manual re-sizing and re-meshing (Aremu et al., 2013). Through the generation of novel designs, which could result from new AM capabilities, designers are prompted to think beyond their prior experience and bias, often related to conventional fabrication approaches, and explore novel solutions.

Using the example of a car wheel design, this paper defines a spatial grammar for the wheel spoke design generation that encodes the fabrication constraints for the Fused Deposition Modeling (FDM) process based on the UPrint SE Plus machine. A related paper (Chen, Stöckli and Shea, 2015) details the testing of such constraints including achievable dimensions, feature spacing and angles for this type of printer. The resulting spatial grammar models these constraints in addition to the style of the designer and, thus, only designs in the language of the AM process and defined style are generated. The spatial grammar is then used to explore the design space and generate both known and novel designs, some of which are printed directly as examples. Finally, the automated link to simulation using the Finite Element Method is shown as an initial step towards future research connecting generation with simulation and optimization.

1.1 Background

1.1.1 Spatial grammars

Design synthesis is a process where the designer creates form and structure that possess the required behavior and function (Starling and Shea, 2005). The first step involves the creation of elementary components that may be used in insolation or combination during synthesis. The conceptual design process is commonly carried out on an ad-hoc basis based on human creativity (Antonsson and Cagan, 2001). By formalizing this process, one can leverage computational power in generating designs on a semi- or fully-automated basis. Three major approaches developed in this field are function-based synthesis, grammar-based synthesis and analogy-based design (Chakrabarti et al., 2011). A grammar-based synthesis method, in particular parametric spatial grammars, is adopted in this research. Stiny (1980) defines the spatial grammar formalism as a transformation of the current working shape (CWS) γ by replacing a subshape $\tau(\alpha)$ with subshape $\tau(\beta)$, i.e. $\gamma' = [\gamma - \tau(\alpha)] + \tau(\beta)$, according to a set of pre-defined rules $\alpha \rightarrow \beta$. This can be thought of as matching shapes on the left hand side (LHS) and replacing those shapes with the shapes on the right hand side (RHS) under the transformation τ.

As the design task in this paper focuses mainly on spatial design for style, Agarwal and Cagan (1999) originally show the ability of spatial grammars to encode particular styles in product design through the example of coffee makers. Creating the link between generative design and fabrication, Sass (2006) describes a Digital Design Fabrication (DDF) process as a series of stages including conceptualization, materialization and fabrication. In particular, he recommends rule-based generative methods for the conceptualization phase and AM for materialization and fabrication. This approach is taken in the automated design generation of different truss configurations of grid dome structures. The truss members with unique structural joints are fabricated using FDM (Sass, 2008) and manually assembled to give constructionist visualizations. Two areas of improvement are identified, 1) the spatial grammar is used to generate a symbolic representation of the geometry instead of the solid geometry itself, and the actual model is built during post-processing, 2) the customization is mainly focused on the arrangement of the members, i.e. the assembly instead of individual components, where only the lengths varied. Both points are addressed in this paper.

While in the original shape grammar work most rules were defined and applied only on paper or in 2D space, there have since been a few 3D computational implementations. Hoisl and Shea (2011) provide a comprehensive overview of spatial grammar implementations. McKay, et al., (2012) discuss the various implementations of spatial grammars and the feature set of each.

One implementation developed, Spapper, by Hoisl and Shea (2011) is adopted here for the wheel rim generation. Spapper is implemented as an add-on (workbench) for FreeCAD, an open-source CAD system based on the open-source geometric modeling kernel OpenCascade. Primitives such as rectangular prisms, cylinders, cones, spheres, torus, ellipsoids, and helices are used to define the grammar vocabulary. Thus, it is, more specifically, a set grammar implementation of a spatial grammar. The rules may be implemented parametrically, enabling both parametric rule detection (LHS), and parametric rule replacement (RHS). Labels are used to carry persistent variables, to simplify the matching process and their coordinates and orientations may also be parametric (Hoisl and Shea, 2013). A detailed account of the algorithms behind and the capabilities of Spapper may be found in Hoisl's doctoral thesis (2012).

1.1.2 DfAM Constraints

A series of test specimens are printed on a uPrint SE Plus FDM machine to determine the minimum dimensions, spacing and angles that can be fabricated (Chen, Stöckli and Shea, 2015) to an acceptable quality as compared to the CAD model. A summary of the dimensions relevant to the design task in this paper are listed in Table 1 and they are incorporated into the spatial grammar rules prior to design generation. Further details of the testing can be found in Chen et al. (2015).

Table 1. Relevant additive manufacturing constraints on uPrint SE Plus

Dimensions	**Range of validity**	**Comments**
Minimum width in the horizontal direction	$w \geq 2.0$ mm	1.0 mm if not structural
Minimum thickness in the vertical direction	$h \geq 0.66$ mm	Equivalent of two layers
Minimum spacing in the horizontal direction	$s_{\mathrm{h}} \geq 0.1$ mm	
Minimum interior / exterior angle	$\alpha_{\mathrm{I}} \geq 10.0°$	
Angle of overhang to eliminate support material	$\theta_{\mathrm{OH}} \geq 45°$	For $t_{\mathrm{Layer}} = 0.0254$

2 DESIGN TASK

The design of car wheels is divided into the design of the spokes, the hub and the rim. Wheel spoke design is a suitable design challenge to illustrate the research since it involves both functional and aesthetic criteria as well as offers a large number of potential variations. This paper focuses on the arrangement and design of the spokes; the rim and the hub are inserted for analysis purposes and remain invariant in design generation. The spatial grammar rules are developed based on a qualitative study of real automotive wheel rims with the intention of generating both known and unexpected designs. The spatial grammar presented here results from a survey of various rim designs from automotive manufacturers and builds on a similar exercise done as the initial example in Hoisl's thesis (2012). The aim here is to incorporate DfAM constraints, allow automated design generation that was not previously considered, and to provide an automated link to FEM. The particular wheel design task here is also different than Hoisl (2012) and is part of a balloon powered model car assembly designed specifically for 3D printing as described in Chen et al. (2015). Only symmetric designs are considered but this constraint could be relaxed in the future. The overall size of the assembly dictates that the wheel spokes are dimensioned in the meso range, i.e. $0.1 \rightarrow 10$ mm. The scale in relation to the printing process compels designers to consider fabrication constraints.

In addition to the general DfAM constraints defined in Table 1, specific constraints are imposed as well to produce customized wheel designs that are guaranteed valid, i.e. directly printable on the uPrints. The constraints are 1) the hub must be connected to the rim without interruption, and 2) the model must be completely manifold for FEM meshing and 3D printing; in particular, shared edges cannot exist, i.e. the red line in Figure 1.

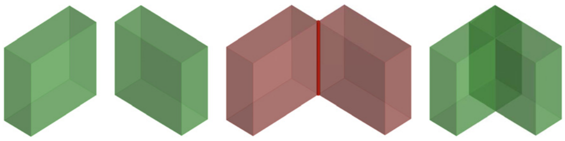

Figure 1. Manifold criterion example where the red line in the center example indicates a shared edge only between two solid geometries and thus violating the manifold constraint.

3 SPATIAL GRAMMAR RULES

The development of the spatial grammar results in defining 10 parametric shape rules that are described in this section. The rules are grouped into two sets; the first set involves topologic changes to the spokes and the second set applies surface finishing to existing spokes. Attention is primarily paid to the Right Hand Side (RHS) portion of the first set of rules, five in total, in particular, the parametric dimensions and orientations of the rectangular prism (box) members within.

To give an overview of the grammar, the first rule (Table 2) generates a single spoke between the hub and the rim. Rule 2 (Table 3) adds an additional spoke at an angle α to the original. Rule 3 (Table 4) adds a pitch (out of plane) angle β to a spoke. Rule 4 (Table 5) splits a spoke into two and reverses the pitch angle of the outer segment, if necessary. Rule 5 (Table 6) splits the outer segment into two segments with an angle γ in between. Additional rules are developed to add surface finishing to existing spokes.

3.1 Rule 1 – Initial spoke and persistent parameter definition

The wheel spokes are envisioned to be a design that radially expands outward from a central hub. The first rule starts at the hub indicated by a starting symbol and defines one continuous spoke from it to the rim. Though not efficient by any means, Rule 1 generates a starting valid solution that already satisfies all the constraints.

In addition to the generation of the spoke, Rule 1 also defines all the subsequent parameters that need to be carried throughout the generation process. The aforementioned constraints (Table 1) are integrated into the allowable range of these parameters. To produce aesthetically conventional wheels, it is specified that each design should be symmetric about each spoke. To achieve symmetry, the parameters must be made persistent throughout the generation process. This is an extension of Oberhauser et al.'s (2014) initial shape variables in that these persistent variables are replicated and transformed with the application of each rule for each resulting member, giving them geometrical significance as well. In this implementation, labels are the only elements able to carry this information. Table 2 shows the free parameters associated with each geometry and label and the range of each parameter. Note that some parameters are discrete and may have step sizes greater than one.

The dimensions of the strut follow the minimum dimension constraints. The minimum width is $w = 2$ mm, and the minimum thickness is set at $h = 1$ mm. To ensure continuity, length is fixed at the distance between the center of the hub to the edge of the rim, $l = 13.5$ mm. The spoke angle α is defined as $\alpha = 360/n$. With a minimum angle of $\alpha = 10°$, 36 spokes may fit around the hub. To limit this, a maximum number $n_{\max} = 20$ spokes is set. The pitch defines the angle at which spokes extend from the hub to the rim. To avoid support structure under the spokes, a minimum pitch of 45° must be set if the wheel were to be printed horizontally. This pitch angle would extend beyond the envelope of the rim and produce non-sensible designs. Therefore, the overhang constraint is relaxed. Should a spoke be split into inner and outer portions, an inner length l_i is defined. The outer portion may be further split in the yaw direction. γ is defined as half of the split angle and its range is set from 5° to 85°. Width of the split outer spokes is defined by w_o, and ranges from 2 mm to width of the original spoke.

Table 2. Parametric definition of rule 1

Rule definition

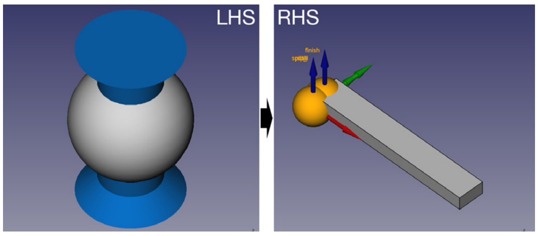

Sample resulting shape

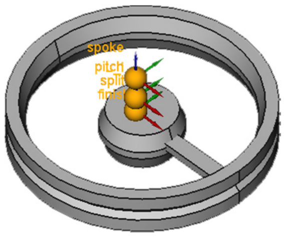

LHS		
Starting symbol		
RHS		
	Min Value	**Max Value**
Box		
Length l	13.5	
Width w	2.0	5.0
Height h	1.0	2.0
Label.spoke		
# spoke n	3	20
Label.pitch		
Pitch β *(in step size* 5°*)*	0	30
Label.l_i		
Inner length l_i	l_i *(see Rule 4)*	
Label.split		
Split angle γ	1	8
Split width w_o	2	w
Label.final *(for hub and rim insertion)*		

3.2 Rule 2 – Generation of subsequent spokes

Rule 2 inserts spokes at an angle α to the neighboring spoke where α is defined as the angle between two adjacent spokes. This rule is applied $n-1$ times where n is the number of spokes. α is a persistent parameter defined in rule 1 and retrieved from *Label.spoke*.

Table 3. Parametric definition of rule 2

Rule definition

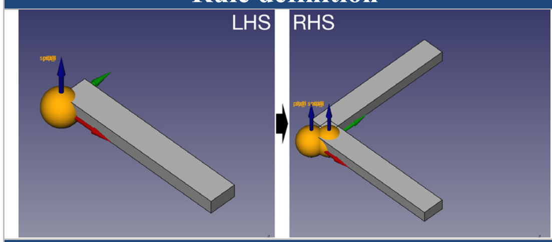

Sample resulting shape

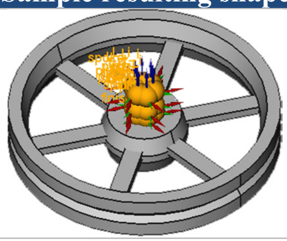

LHS	
Label.spoke	
Box	
RHS	
Label.spoke1, .split1, .L_i1, .pitch1, Box1	
TranslateX	0
TranslateY	0
Label.spoke2, .split2, .L_i2, .pitch2, Box2	
TranslateX	$\Delta x = w/2 \sin \alpha$
TranslateY	$\Delta y = w/2\,(1 - \cos \alpha)$

As the rotation is centered on the origin (lower left corner) and not the center of the spoke end, an offset must be applied to the new spoke as to not generate non-manifold designs. All labels except *Label.spoke* are copied to the origin of the new spoke, whereas *Label.spoke* is deleted from the original position and moved. These offsets are applied to the labels as well. The offsets are decomposed into the rule coordinate system and applied as equations to the free variables *TranslateX* and *TranslateY*. Note that these quantities depend both on the width of the spokes w and the angle of rotation α.

3.3 Rule 3 – Add a pitch angle to a spoke

To an otherwise flat 2D design space, Rule 3 pitches the spokes up by the angle β. Note that with a large enough β, the spokes may not come in contact with the rim. This violates the manifold constraint and must be remedied with Rule 4. To ensure that the pitched spokes are still able to maintain the manifold constraint with the rim for Rule 4, i.e. overlapping it, the projected length is equal to the original length (Figure 2). Figure 2 shows the sequence of transformations that take place. Step 2 assigns a pitch β to the spoke and step 3 extends the spoke so that its projection on the x-y plane covers the same length as the original spoke.

Table 4. Parametric definition of rule 3

<table>
<tr><th>Rule definition</th><th colspan="2">LHS</th></tr>
<tr><td rowspan="7">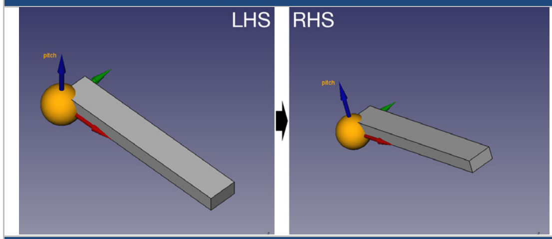
</td><td colspan="2">Label.pitch</td></tr>
<tr><td colspan="2">Box</td></tr>
<tr><td colspan="2">RHS</td></tr>
<tr><td colspan="2">Label.pitch</td></tr>
<tr><td>Pitch</td><td>β</td></tr>
<tr><td colspan="2">Box</td></tr>
<tr><td colspan="2"></td></tr>
<tr><td>Sample resulting shape</td><td>Length</td><td>$l_{\text{new}} = l/\cos\beta$</td></tr>
<tr><td rowspan="2">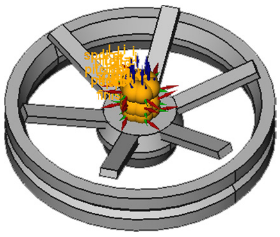</td><td>Pitch</td><td>β</td></tr>
<tr><td colspan="2">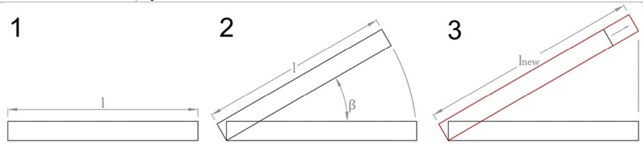

Figure 2. Transformation of rule 3</td></tr>
</table>

3.4 Rule 4 – Spoke section-wise split

Rule 4 splits one spoke into an outer and an inner segment along its cross-section and rotates the outer spoke back in the pitch direction by $-\beta$. Refer to Figure 3(L), continuity is no longer maintained for a spoke above a certain β, therefore the portion of the spoke that extends beyond the wheel bounding box must split at or before the box and be rotated back. The $l_{\mathrm{i,max}}$ in Figure 3(L) indicates the maximum inner segment length possible for that particular pitch angle $\beta_{\max}$. The inner spoke length l_{i} defines the split location in a spoke. An empirical formula derived from the polynomial fit in Figure 3(R) is used to define the maximum inner spoke length as a function of β. For pitch angles that do not cause discontinuity, a maximum inner length of $l = 13.5$ mm is used.

$$l_{\mathrm{i}}(l, \beta) = \mathrm{rand}[0, \min(l, -0.0002548\beta^3 + 0.03015\beta^2 - 1.268\beta + 22.72)] \tag{1}$$

Equation 1 states that the inner length is a uniform random number between 0 and the lesser of the whole length or the intersection point defined by the empirical formula. The greater the pitch angle is, the more likely it will be for the split to occur near the hub, and vice versa. The corollary is that a split cannot occur outside of the blue line as that would result in a discontinuous geometry.

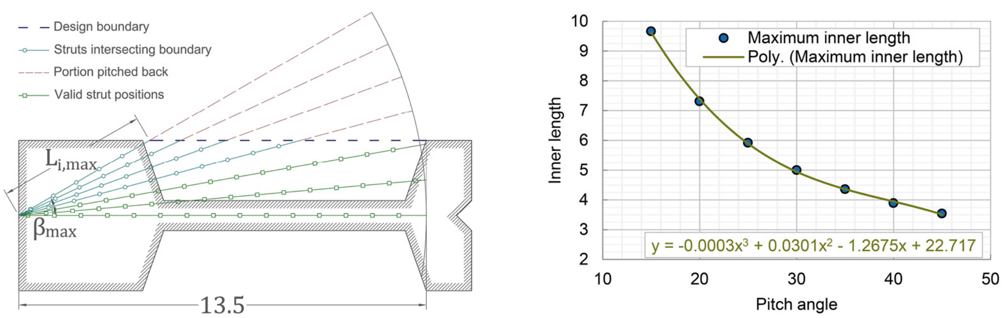

Figure 3. Allowable spoke pitch angles (L), polynomial fit of location of splitting (R)

The outer spoke is rotated by angle β. To ensure that the model remains manifold, the outer spoke is then shifted back by $(\Delta x, \Delta y)$ to overlap with the inner spoke. The height of the outer spoke h_{o} is reduced so that the surface transitions are continuous on both sides. Note that since this rule may be applied to spokes with any pitch, the transformation rule does not assume a fixed coordinate system.

Table 5. Parametric definition of rule 4

<table>
<tr><th>Rule definition</th><th colspan="2">LHS</th></tr>
<tr><td rowspan="7">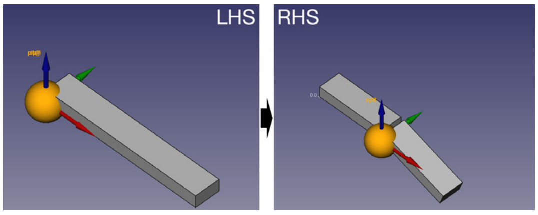
</td><td colspan="2">Label.split, Box</td></tr>
<tr><td colspan="2">RHS</td></tr>
<tr><td colspan="2">Label.split</td></tr>
<tr><td>TranslateX</td><td>$\Delta x = l_{\mathrm{i}} - h\cos\beta\sin\beta$</td></tr>
<tr><td>TranslateY</td><td>$\Delta y = h\cos\beta\sin\beta\tan\beta = h\sin^2\beta$</td></tr>
<tr><td>pitch</td><td>$-\beta$</td></tr>
<tr><td colspan="2">Box1</td></tr>
<tr><th>Sample resulting shape</th><td>Length</td><td>$l_1 = l_{\mathrm{i}}$</td></tr>
<tr><td rowspan="6">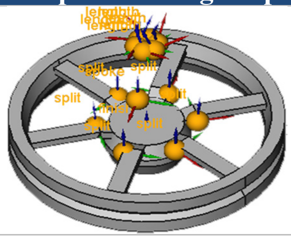</td><td colspan="2">Box2</td></tr>
<tr><td>Length</td><td>$l_2 = l - l_{\mathrm{i}}$</td></tr>
<tr><td>Height</td><td>$h_2 = h\cos\beta$</td></tr>
<tr><td>TranslateX</td><td>$\Delta x = l_{\mathrm{i}} - h\cos\beta\sin\beta$</td></tr>
<tr><td>TranslateY</td><td>$\Delta y = h\sin^2\beta$</td></tr>
<tr><td>pitch</td><td>$-\beta$</td></tr>
</table>

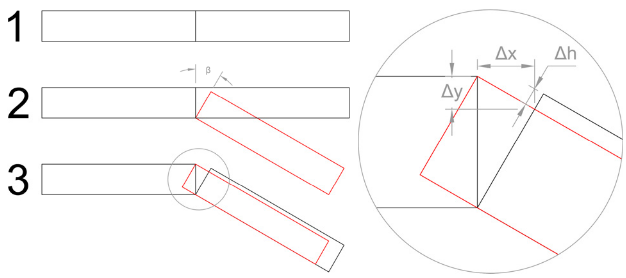

Figure 4. Steps illustrating the transformation of Rule 4

3.5 Rule 5 – Outer segment of a spoke, length-wise split

Rule 5 splits the outer segment of a spoke length-wise into two mirroring segments with angle γ in between. The persistent variables needed are the width of the split struts w_{o}, and the angle of split γ; both of which are carried through with labels. To ensure continuity, the rotated segments are then lengthened so that the end surface is fully embedded in the rim. Two additional labels are added on the RHS at the local origin of each resulting spoke for subsequent rules.

$$l_{\mathrm{o}} = (l - l_{\mathrm{i}})\frac{\sin\left[\gamma - \sin^{-1}\left(\frac{l_{\mathrm{i}}}{l}\sin\gamma\right)\right]}{\sin\left(\frac{l_{\mathrm{i}}}{l}\sin\gamma\right)} + \frac{w_{\mathrm{o}}}{2}\frac{l_{\mathrm{i}}}{l}\sin\gamma \qquad (2)$$

Figure 5 shows that a simple rotation would result in an asymmetry that violates the continuity constraint (step 2). A linear transformation is applied to shift the center of the two outer struts to coincide with the center of the inner strut (step 3). A length extension is applied to both outer struts to ensure that they overlap with the rim (step 4). The new length is defined in Equation 2, the deviation of which follows the geometry shown in Figure 5. Where due to the center of rotation being shifted to the location of split as opposed to the hub, the split spoke must be lengthened.

3.6 Rule Set 2: Surface Treatment and Clean-Up

Rule set 2 consists of seven rules that apply minor changes to the existing spokes. The first four rules apply edge filleting of different radii to spokes that have thicknesses greater than 2 mm. One rule splits a spoke with a minimum width of 2 mm into two parallel spokes. Finally, three rules remove the labels that are still present in the CWS for visualization purposes and geometry export. The rules are not presented here specifically due to space restrictions.

Table 6. Parametric definition of rule 5

Rule definition

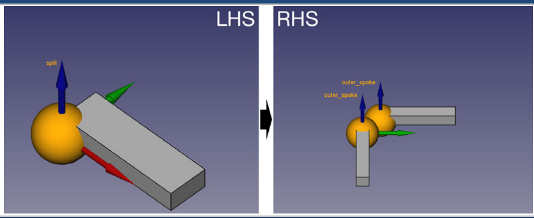

Sample resulting shape

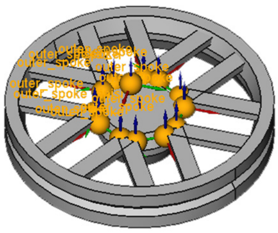

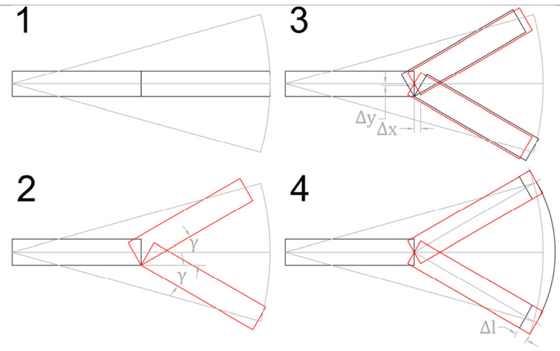

Figure 5. Steps of transformation

LHS	
Label.pitch	
Box	
RHS	
Label.outer_spoke1	
Yaw	γ
TranslateX	$\Delta x = -w_o/2\cos(\gamma)$
TranslateY	$\Delta y = w_i/2 - w_o/2\sin(\gamma)$
Box1	
Length	$l_o = f(l, l_i, \gamma, w_o)$
Width	w_o
Yaw	γ
TranslateX	$\Delta x = -w_o/2\cos(\gamma)$
TranslateY	$\Delta y = w_i/2 - w_o/2\sin(\gamma)$
Label.outer_spoke2	
Yaw	$-\gamma$
TranslateX	$\Delta x = w_o/2\cos(\gamma)$
TranslateY	$\Delta y = w_i/2 + w_o/2\sin(\gamma)$
Box2	
Length	$l_o = f(l, l_i, \gamma, w_o)$
Width	w_o
Yaw	$-\gamma$
TranslateX	$\Delta x = w_o/2\cos(\gamma)$
TranslateY	$\Delta y = w_i/2 - w_o/2\sin(\gamma)$

4 RESULTS

Accounting for all possible topologic and parametric variations, and restricting the persistent parameters to only integers, Rule Set 1 is able to generate 72,500 valid designs. Of these valid combinations, 100 designs are automatically generated, 15 of which are shown in Table 7. The value of the parameters listed in Table 2 to Table 6 are either generated randomly or calculated based on the randomly generated numbers. Row A of Table 7 presents designs similar to real rim designs from automotive manufacturers. Row B shows designs with additional surface finishing using Rule Set 2. Row C illustrates designs that are unusual and unlikely to be conceived by human designers. Row D shows five fabricated designs as proof-of-concept that the designs generated are directly printable on the UPrint SE plus as modeled.

It is evident that one can cover a large range of existing designs with a few basic rules. Further, these rules are able to generate a number of sensible yet unexpected, designs that are complex and intricate all the while conforming to the design style encoded and fabrication, i.e. DfAM, constraints.

5 DISCUSSION

This paper describes the automated generation of valid car wheel spoke designs for 3D printing using UPrints through the development and application of a 3D, parametric spatial grammar. It shows that with a limited rule set, one can define and explore a large design space that reflects both the defined style and AM constraints. The rules developed may be customized to fit a particular brand image, visual aesthetics and functional criteria. Conversely, the user is also able to choose designs that fit their expectations from a large pool. In comparison to parametric modeling, not all combinations of parameters must be thought of *a priori* thus providing a richer representation and more direct modeling approach. In principle, one could 3D print all 72,500 valid designs without the need for tooling or CNC coding, thus highlighting the synergy between generative design via spatial grammars and the capability of 3D printing to fabricate unique and customized designs. Further, the designs generated already meet the AM constraints modeled without the need for post-processing or paper-based guidelines. The design tool could also be made accessible online for customers to generate their own designs automatically or interactively.

Table 7. Design variants automatically generated and their fabricated counter-parts

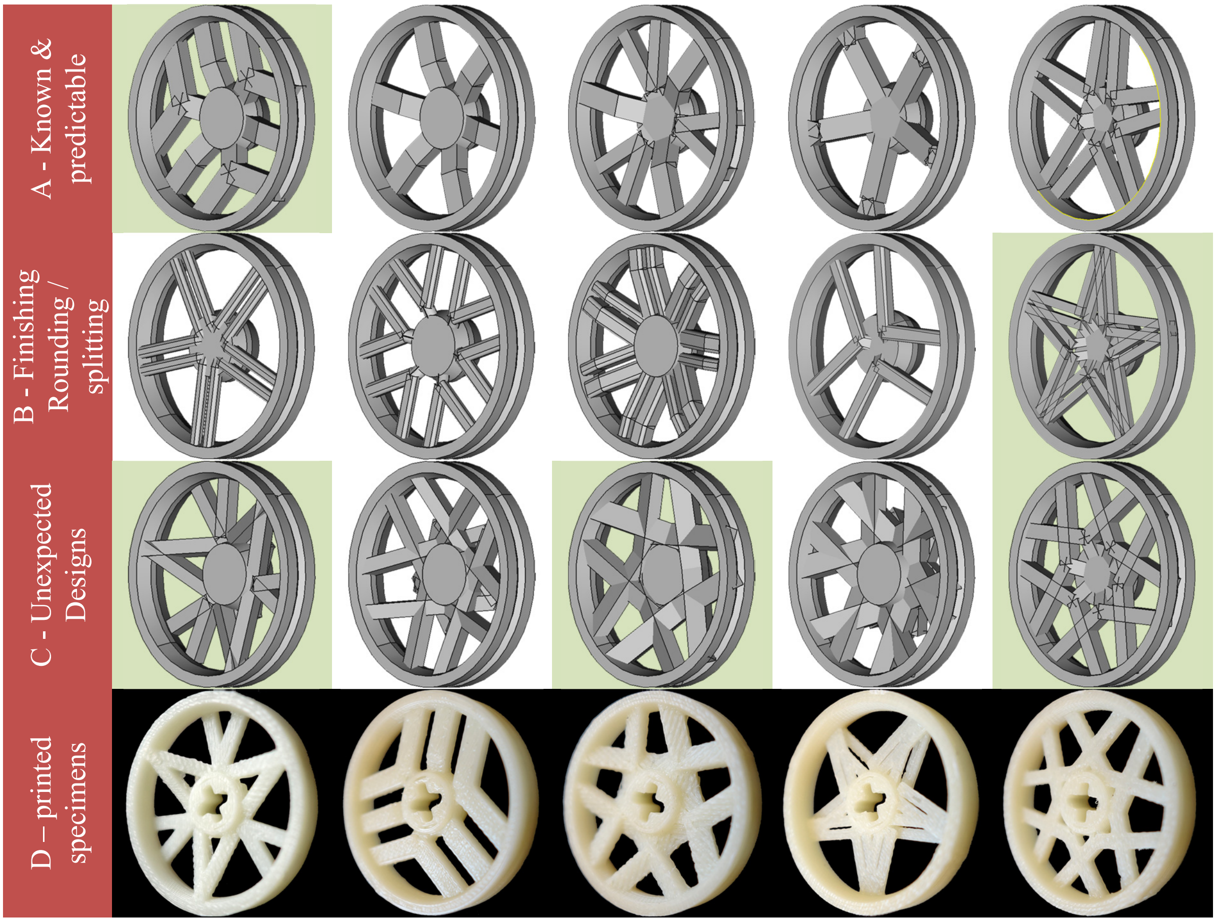

To further automate the selection process, as each generated design is automatically meshable due to the manifold constraint, the wheels may be analyzed automatically with FEM. The automation is further simplified by the fact that both boundary and load conditions are applied to components that are invariant, i.e. the hub and the rim respectively (Figure 6(C)). The results may be evaluated based on a variety of criteria, for example, least compliant and lowest drag coefficient.
To demonstrate this, a selected design is meshed with GMSH and analyzed linear elastically with Abaqus. The loading condition simulated is a radially inward uniform pressure on a third of the rim; the axle is assumed to be pinned. The mesh and the principal strain are shown in Figure 6 (L and R).

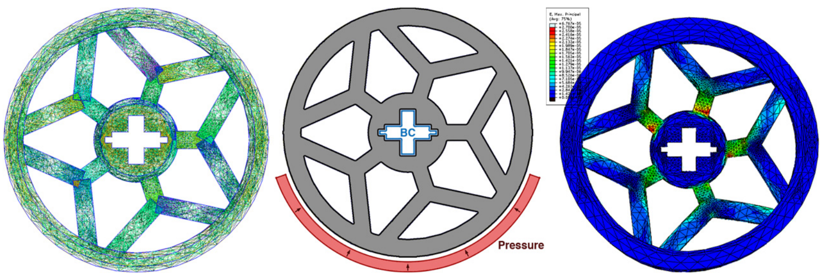

Figure 6. Mesh (L), BC / LC (C) and the resulting principal strain diagram from Abaqus (R)

6 CONCLUSION

Computational design-to-fabrication is introduced in this paper and aims to take advantage of new opportunities in AM by computationally encoding the constraints of AM processes, in addition to other considerations like style and engineering performance, in generative design systems that automatically and interactively generate and optimize designs that are directly printable. This paper discusses specifically the adoption of spatial grammars to automatically generate car wheel spoke designs that conform to DfAM constraints as well as FEM meshing and analysis requirements. Two sets of 3D, parametric spatial grammar rules are developed to define and explore the design space. These rules incorporate fabrication constraints in their dimensional parameters so that the designs are guaranteed valid. 72,500 valid designs may be generated with integer value parameters and more considering real values. The results show that with these limited sets of rules one is able to reproduce real designs as well as to generate valid, yet unexpected designs. Further steps may be taken to mesh the resulting geometry and carry out FEM simulation as an initial step for future work to integrate automated simulation and optimization.

REFERENCES

Agarwal, M. and Cagan, J. (2000) On the use of shape grammars as expert systems for geometry-based engineering design, Artificial Intelligence for Engineering Design, Analysis, Vol. 14, No. 5, pp. 431-439.

Agarwal, M., Cagan, J. and Constantine, K.G. (1999) Influencing generative design through continuous evaluation: Associating costs with the coffeemaker shape grammar, Artificial Intelligence for Engineering Design, Analysis and Manufacturing, Vol. 13, pp. 253-275.

Antonsson, E.K. and Cagan, J. (2001) Formal engineering design synthesis, 1st ed, Cambridge: Cambridge University Press.

Aremu, A., Ashcroft, I., Wildman, R., Hague, R., Tuck, C. and Brackett, D. (2013) The effects of bidirectional evolutionary structural optimization parameters on an industrial designed component for additive manufacture, Proceedings of the Institution of Mechanical Engineers, Part B: Journal of Eng. Manufacture, Vol. 227, No. 6, pp. 794-807.

Chakrabarti, A., Shea, K., Stone, R., Cagan, J., Campbell, M., Hernandez, N. and Wood, K. (2011) Computer-based design synthesis research: An overview. Journal of Computing and Information Science in Engineering, Vol. 11, No. 2, 021003.

Chen, T., Stöckli, F. and Shea, K. (2015) Design for Mass Customization using Additive Manufacture: Case-Study of a Balloon-Powered Car, To appear: Proceedings of the 20th International Conference on Engineering Design, Milan.

Dimitrov, D., van Wijck, W., Schreve, K. and de Beer, N. (2006) Investigating the achievable accuracy of three dimensional printing, Rapid Prototyping Journal, Vol. 12, No. 1, pp. 42-52.

Doubrovski, Z., Verlinden, J.C. and Geraedts, J.M.P. (2011) Optimal design for additive manufacturing: Opportunities and challenges, Proceedings of the ASME Design Engineering Tech. Conf., pp. 635-646.

Hoisl, F. (2012) Visual, Interactive 3D Spatial Grammars in CAD for Computational Design Synthesis, Munich: Technischen Universität München.

Hoisl, F. and Shea, K. (2011) An interactive, visual approach to developing and applying parametric three-dimensional spatial grammars, AI EDAM, Vol. 25, No. 04, pp. 333-356.

Hoisl, F. and Shea, K. (2013) Three-dimensional labels: A unified approach to labels for a general spatial grammar interpreter, Artificial Intelligence for Engineering Design, Analysis and Manufacturing, Vol. 27, No. 04, pp. 359-375.

McKay, A., Chase, S., Shea, K. and Chau, H.H. (2012) Spatial grammar implementation: From theory to useable software, Artificial Intelligence for Engineering Design, Analysis and Manufacturing, Vol. 26, No. 02., pp. 143-159.

Meisel, N.A. and Williams, C.B. (2014) Design For Additive Manufacturing: An Investigation Of Key Manufacturing Considerations In Multi-Material Polyjet 3d Printing, 24rd Annual International Solid Freeform Fabrication Symposium, Vol. 136, pp. 980-997.

Oberhauser, M., Sartorius, S., Gmeiner, T. and Shea, K. (2014) Computational design synthesis of aircraft configurations with shape grammars, 6th International Conference on Design Computing & Cognition, London.

Sass, L. (2008) Parametric constructionist kits: Physical design and delivery system for rapid prototyping devices, International Journal of Architectural Computing, Vol. 07, No. 04, pp. 623-642.

Sass, L. and Oxman, R. (2006) Materializing design: the implications of rapid prototyping in digital design, Design Studies, Vol. 27, No. 3, pp. 325-355.

Starling, A. and Shea, K. (2005) A parallel grammar for simulation-driven mechanical design, 31st Design Automation Conference, Parts A and B, Vol. 2, pp. 427-436.

Stiny, G. (1980) Introduction to shape and shape grammars, Environment and planning B, Vol. 7, No. November, pp. 343-351.